Published by :
http://www.ijert.org

International Journal of Engineering Research & Technology (IJERT)
ISSN: 2278-0181
Vol. 11 Issue 01, January-2022

Investigation of Turbulent Airflow in a Circular Pipe Using Different Orifice Plate Geometries

Ahmed Ballil
Mechanical Engineering Department
University of Benghazi
Benghazi, Libya

Shaban Jolgam
Mechanical Engineering Department
University of Zawia
Zawia, Libya

***Abstract*—The present paper demonstrates the results obtained from an experimental study of the turbulent airflow through a circular pipe by means of a set of orifices that have different sizes and shapes. Five orifice plates were manufactured and utilized in the investigations; three circular orifice plates of 50 mm, 38 mm, and 25 mm in diameter with square edges; in addition to a triangular and another square orifice plate with the same flow area as the circular orifice plate of 25 mm in diameter. The experiments were carried out using different flow velocities. The results were compared with those obtained for a plain tube at the same flow conditions. It is observed that the size and shape of the orifice as well as the volumetric flow rate have a considerable effect on the pressure drop along the pipe. This finding can be useful in piping system design when losses are taken into account.**

Keywords*—Turbulent flow; circular pipe; orifice plate; flow measurment; pressure drop

I. INTRODUCTION

Turbulent fluid flow through circular pipes is typically encountered in engineering applications. For instance, the water distribution systems and the transportation of natural gas for long distances by large pipelines. These types of flow are associated with a pressure decrease mainly due to friction between fluid layers and the pipe wall, in addition to other minor losses. Therefore, the flow parameters, such as flow rate and pressure drop, need to be considered in designing piping systems and measured continuously while in operating process.

The process of determining fluid flow characteristics in a plant, piping system, ventilation system, or other engineering industry is known as flow measurement. There are a variety of methods and devices that can be utilized to measure fluid flows, such as Coriolis force, differential pressure, vortex shedding, electromagnetic, anemometer, ultrasonic, and positive displacement meters. Among these methods, the differential pressure technique is commonly utilized in fluid flow applications. This method mainly depends on using an orifice meter device, which has the advantages of simple construction, low manufacturing cost, long operating life, and adequate accuracy.

The ordinary orifice meter is simply a thin flat plate with a centrally drilled hole that is machined to a sharp edge. The orifice plate is inserted perpendicular to the flow between two flanges, allowing the flow to pass through the hole in which the flow area is reduced. As the fluid flows through the orifice, where the sharp edge points upstream of the flow, it compresses and then expands, causing a pressure decrease that can be measured across the orifice [1]. Then the volumetric flow rate can be calculated as a function of the discharge coefficient and the differential pressure.

It is expected that the flow meters with different orifice sizes and shapes will have a large effect on the pressure drop measured across them. This, of course, has an effect on pressure loss and turbulence properties on the downstream side of the orifice. Therefore, investigation and analysis of such behavior are supposed to be crucial matters. In the present work, a set of orifice plates with different sizes and shapes are manufactured and then utilized to study the turbulent airflow through a circular pipe experimentally. In particular, the pressure drop along the pipe has been investigated as a function of beta ratio, orifice shape, and Reynolds number. The experiments have been conducted using a nozzle-pipe flow apparatus equipped with a fan set. The airflow velocity can be controlled by setting the rotational speed of the motor's shaft that drives the fan.

The rest of this manuscript is organized as follows: A number of recent research studies on the topic are reviewed in the next section. Then the apparatus specifications and experimental setup are described. After that, the results obtained are presented. Finally, the conclusion is stated.

II. LITERATURE REVIEW

A computational study was carried out to evaluate the efficiency of multiple orifice configurations in producing pressure drops and the effect of compressibility on the pressure drop in [2]. The standard k-ε turbulence model was used to solve the governing equations. According to the CFD results, orifice systems that were utilized in the incompressible flow domain could not be used for high operating pressure ratio flows. The results showed that an orifice area ratio of more than 2.5 caused comparatively large pressure drop. However, the total pressure decrease in the cases of compressible pipe flows via double and triple orifice systems was mostly due to shock losses.

International Journal of Engineering Research & Technology (IJERT)
ISSN: 2278-0181
Vol. 11 Issue 01, January-2022

An experimental study was performed using a swirler flow conditioner in disturbed flows [3]. The experiments were conducted on two rigs using water and airflow. It was proved that the error of metering caused by disturbances could be decreased by utilizing a swirler flow conditioner. For the optimal swirler flow conditioner design, a range of alternative forms was investigated. The cone swirler was found to be the most effective in reducing distortion at high Reynolds numbers. However, it had less effect on swirling flow at a low Reynolds number. A new discharge coefficient for the cone swirler flow conditioner was established for both low and high Reynolds numbers.

Experimental measurements of the pressure drop after fractal-shaped orifices in a turbulent flow pipe were carried out in [4]. The results confirmed that for the identical flow areas of orifices, the pressure drop across the fractal-shaped orifices was lower than the pressure drop across normal orifices. The findings suggest that fractal-shaped orifices could be utilized as flowmeters since they can detect pressure drops after these orifices more precisely than ordinary orifices. However, their sophisticated manufacturing is the main issue.

A multi-hole orifice structural design technique was presented in [5]. This methodology was applied experimentally using water as a working fluid. Initially, the geometric architecture, which included the criteria of orifice arrangement, total orifice number, orifice distribution density, and equivalent diameter ratio, was used to quantify the multi-hole orifice structures. Then the correlation between multi-hole orifices geometric features and the pressure loss coefficient was developed and further simplified using experiments. The final pressure loss coefficient model was extremely precise, demonstrating that the method employed was successful.

The finite volume approach was adopted for the numerical evaluation of the extensional viscosity measured using an orifice flowmeter in [6]. The results were found to be in harmony with available experimental data that had previously been published. Abrupt contractions were used, and flow fields illustrated the formation of vortices and showed dead zones downstream of the orifice. Based on a semi-hyperbolic profile, a novel die geometry was developed and effectively tested with both Newtonian and non-Newtonian fluids.

Computational fluid dynamics was utilized as a tool in the analysis of natural gas flow through a high-pressure pipeline equipped with deformed and undeformed orifice plates [7]. In the computations, it was assumed that the natural gas had the same physical and chemical properties as pure methane. The results showed that the deformation of an orifice plate had a large effect on the stream field in the high-pressure pipeline. Different behaviors in the gas stream were caused by shape deformation. Last of all, the results revealed that if the deformation was not taken into account when calculating the final volumetric flow, the accuracy of the measurement could be exaggerated.

In [8], the porosity of a fractal flow conditioner was experimentally analyzed concerning the accuracy of the orifice plate flowmeter. The optimal distance of the fractal flow conditioner upstream of the orifice plate flowmeter was identified. In the experiments, several porosities of fractal flow conditioners were mounted at various distances upstream of the orifice plate in conjunction with various disturbances to analyze the effects of these devices on mass flow rate measurement. The results revealed that with a lower value of the fractal flow conditioner, there is an increase in pressure drop and a change in the discharge coefficient of the orifice. According to the comparisons with past results, the fractal flow conditioner was capable of maintaining metering accuracy up to the level needed in the standards.

Dandwate et al. [9] conducted a numerical and experimental study on the influence of orifice plate shape on the coefficient of discharge. The performance of different orifice geometries was compared using turbulence models and CFX as a computational solver. Numerical computations were performed based on a single-hole orifice plate and a set of multi-hole orifice plates consisting of five, seven, and nine holes, respectively. Both experimental and numerical results showed that the orifice plate with seven holes had the best performance compared to other orifice plates considered. However, the results obtained from the simulations for the discharge coefficient were higher than those acquired from experiments. This was justified by the losses in the actual fluid flow because of friction, leakage, and fluid contaminants.

Likitha et al. [10] numerically investigated the behavior of concentric orifice meters for a wide range of Reynolds numbers, changeable beta ratio, and varied geometries of the orifice plate. The computations were done with the STAR CCM+ computational fluid dynamics software. The results were consistent with published data, ISO standards, and the data handbook in terms of discharge coefficient, velocity profiles, and pressure profiles. It was concluded that the computational fluid dynamics method could be utilized effectively for estimating discharge coefficients.

Recently, a study of the uncertainty variation of a practical fiscal orifice measurement system used in a natural gas exportation station in Algeria was performed [11]. The uncertainty of the orifice metering station according to the variation in pressure and temperature was assessed. The uncertainty calculation was conducted using the Norwegian Society for Oil and Gas Measurement NFOGM Software. The measurements confirmed that the seasonal variations in temperatures and pressures had a significant effect on the uncertainty.

III. EXPERIMENTAL SETUP

A. Test Rig

The airflow pipe apparatus allows for comprehensive studies of turbulent airflow in pipes equipped with nozzles, orifices, and bends. The apparatus consists of a smooth-walled aluminum alloy pipe of 76 mm in diameter and 6 m in

International Journal of Engineering Research & Technology (IJERT)
ISSN: 2278-0181
Vol. 11 Issue 01, January-2022

length, connected by the suction eye of a centrifugal fan as shown schematically in Fig. 1. Air enters the pipe through a polished nozzle of elliptical form with a 75mm diameter. Beyond the nozzle, there are 14 piezometer taps at close intervals along the pipe. The discharge from the fan can be varied using a slide valve to give a range of air velocity in the pipe of up to about 40 m/s, corresponding to Reynolds Numbers up to 200,000. The fan is belt-driven by a 1 hp 3-phase AC motor. The nominal motor speeds are variable from 0 to 4000 rev/min. The apparatus is connected to a suitable multi-tube manometer having 20 tubes at a 38 cm gauge length for pressure readings in centimeters of water.

B. Geometry of Orifice Plates

In this work, five different orifice plates were utilized for the investigations. The orifice plates were manufactured locally with the same thickness, but they have different sizes and shapes. Three circular orifice plates, with diameters of 50 mm, 38 mm, and 25 mm, were made with square edges. A triangular and another square orifice plate were manufactured with flow areas equivalent to that of the circular orifice plate of 25 mm in diameter. Fig. 2 shows schematic drawings for sharp-edged and square-edged orifices, respectively. Fig. 3 illustrates the front views of the five square-edged orifice plates that were considered in the experiments.

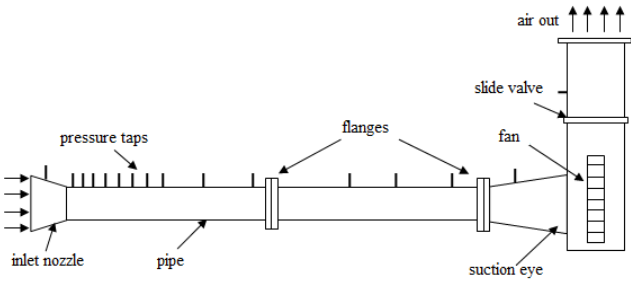

Fig. 1. Schematic drawing for airflow and nozzle apparatus.

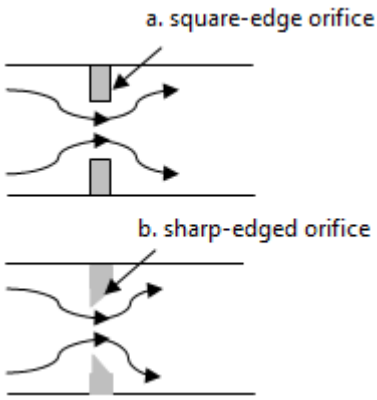

Fig. 2. Schematic illustration of (a) square-edged orifice and (b) sharp-edged orifice.

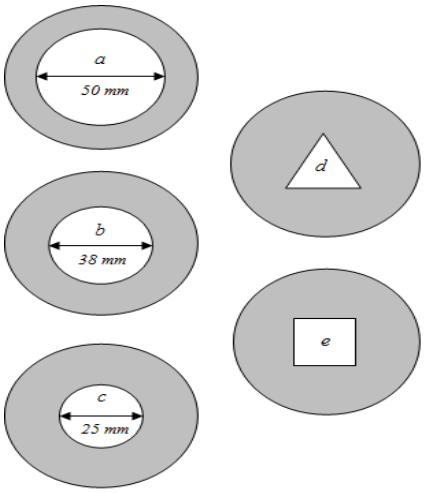

Fig. 3. Different orifice sizes and shapes (a) 50 mm diameter square-edged circular orifice (b) 38 mm diameter square-edged circular orifice (c) 25 mm diameter square-edged circular orifice (d) triangular orifice and (e) square orifice.

C. Sequence of Experiments

A series of experiments have been conducted using the airflow apparatus. The first set of experiments included the investigation of turbulent airflow through a plain pipe at five different motor speeds of 1600 rpm, 2000 rpm, 2400 rpm, 2800 rpm, and 3200 rpm, with a full open slide valve of 100%. The results obtained from this set of experiments have been considered as reference data for further comparisons.

The second set of experiments has been carried out using the different orifice plates, which were fixed behind the inlet nozzle straight away. In each run, one orifice plate was fixed, and the motor speed was set at a constant speed. Three motor speeds of 1600, 2400, and 3200 rpm were considered for each orifice plate, and the slide valve was set to the fully open position.

The flow is started in the pipe by turning on the fan, then left for a short time to ensure the stability of the airflow. In each experimental run, numerous measured pressure differences, h, in centimeters of water, were recorded. Each experiment was repeated three times, measurements were taken, and the average was determined to prevent the influence of the fluctuating flow along the pipe.

D. The Key Measuring Parameters and Main Equations

As mentioned above, the following geometric parameters and flow measurements were considered to quantify and characterize the turbulent flow through the pipe flow apparatus.

- The orifice size is characterized by the beta ratio β, which represents the ratio of a circular orifice diameter to the pipe diameter.
- The orifice shape, where three different orifice shapes that have the same flow area are considered.
- The Reynolds number of the flow is based on the pipe diameter.

International Journal of Engineering Research & Technology (IJERT)
ISSN: 2278-0181
Vol. 11 Issue 01, January-2022

- The pressure drop along the pipe is for each orifice plate.

For the sake of simplicity, it is worth mentioning that since the air velocity at no point exceeds that which corresponds to a Mach number of 0.3, compressibility effects have been neglected in calculations.

When a pressure difference P is small enough to ignore compressibility, the velocity U developed by gas expanding freely from rest under the influence of P is given by:

$$\frac{\rho U^2}{2} = P \quad (1)$$

In the current work, as the pressure difference is measured in centimeters of water, where 1 cmH_2O is equal to 98.1 N/m^2, equation (1) becomes:

$$\frac{\rho U^2}{2} = 98.1h \quad (2)$$

where h represents the drop in static pressure across the nozzle or orifice measured in centimeters of water.

The density of air under atmospheric pressure P_a, and at room temperature T is given by the perfect gas equation:

$$\rho = \frac{P_a}{RT} \quad (3)$$

where R is the universal gas constant which has the value of 287 J/kg.^{o}K.

By combining equations (2) and (3), we get the following relation for flow velocity:

$$U = 237.3\sqrt{\frac{hT}{P_a}} \quad (4)$$

The volumetric flow rate at inlet atmospheric conditions is then given by:

$$Q = k\left(\frac{\pi d^2}{4}\right)237.3\sqrt{\frac{hT}{P_a}} \quad (5)$$

where k is the discharge coefficient of the nozzle or orifice, and d is the diameter. For the present experiments, the value of k is equal to 0.96 for the nozzle as supplied by the vendor. Similarly, the mass flow rate at inlet atmospheric conditions is then given by:

$$\dot{m} = k\left(\frac{\pi d^2}{4}\right)0.827\sqrt{\frac{hP_a}{T}} \quad (6)$$

In all cases, the upstream pressure is always equal to the atmospheric pressure. The pressure tap in the parallel part of the nozzle is used to measure the downstream pressure in the case of nozzles. In the case of the orifices, it is measured at the first tapping in the pipe wall downstream of the orifices. The discharge coefficient k for the orifice plates has been calculated as a function of the beta ratio and Reynolds number using the following formula as given in [12]:

$$k = 0.5959 + 0.0312\beta^{2.1} - 0.184\beta^8 + 0.0029\beta^{2.5}\left(\frac{10^6}{Re_D}\right)^{0.75} + 0.09L_1\beta^4(1-\beta^4)^{-1} - 0.0337L_2\beta^3 \quad (7)$$

where $L_1 = (l_1/D)$ is the distance from the upstream tapping to the upstream face of the plate divided by the pipe diameter and $L_2 = (l_2/D)$ is the distance from the downstream tapping to the downstream face of the plate divided by the pipe diameter. It is recommended that when the value of L_1 is greater than 0.433, the value of 0.039 should be used for the coefficient of the fifth term on the right hand side of (7).

The standard equation connecting pressure drop ΔP over a length of L of straight pipe that has a diameter D takes the form:

$$\Delta P = 4f\left(\frac{L}{D}\right)\left(\frac{\rho U^2}{2}\right) \quad (8)$$

This equation can be rewritten in terms of pressure drop expressed as h in cmH_2O per meter length of pipe as follows:

$$h = \frac{(4f/D)(\rho U^2/2)}{98.1} \quad (9)$$

The friction factor can also be calculated as a function of the Reynolds number for a smooth tube using the well-known Blasius semi-empirical equation as follows:

$$f = 0.316 \times (Re)^{-0.25} \quad (10)$$

IV. RESULTS AND DISCUSSION

First, a series of experiments were carried out on the flow through the plain pipe at a fully opened valve position and using different motor speeds. The obtained results from this set of experiments are illustrated in Figs. 4 and 5.

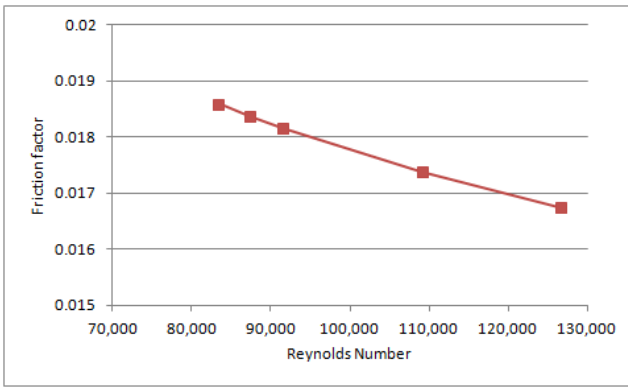

Fig. 4. Variation of the friction factor as a function of the Reynolds number.

International Journal of Engineering Research & Technology (IJERT)
ISSN: 2278-0181
Vol. 11 Issue 01, January-2022

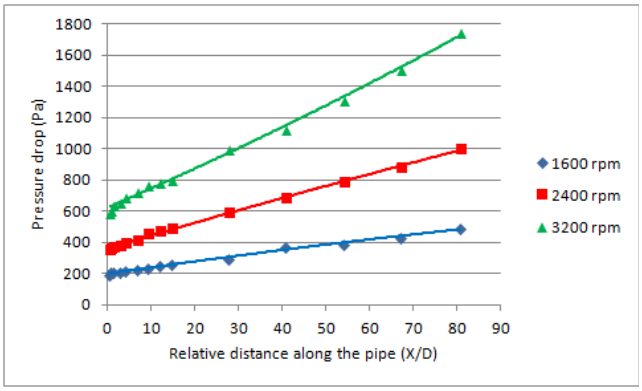

Fig. 5. Pressure drop along the pipe at different airflow velocities

Fig. 4, represents the relationship between friction factor and Reynolds number, where the curve is obtained using the Blasius semi-empirical equation (10). The data for these experiments were collected at five different motor speeds of 1600, 2000, 2400, 2800, and 3200 rpm.

Fig. 5, shows the variations in pressure along the length of the pipe for various motor speeds of 1600, 2400, and 3200 rpm, which produced Reynolds numbers of 83307, 91498, and 12649, respectively. It can be observed that as the motor speed increases, which means the velocity of airflow increases accordingly, the pressure drop increases as well. These curves show the influence of increasing the airflow Reynolds number on the pressure drop clearly. This set of data was considered as reference data for further investigations and comparisons.

The second group of experiments was conducted using different concentric circular orifice plate sizes that were located at the same position behind the inlet nozzle directly. The obtained results are presented in Figs. 6 to 8 for three motor speeds. Obviously, these results show the influence of the beta ratio on the pressure drop along the circular pipe. It can be seen that as the beta ratio decreases, the pressure drop along the pipe increases. It can be noticed that the pressure drop curve increases sharply in the region straightaway downstream of the orifice, then the curve rises gradually in the region further away from the orifice. It is also clear that as the airflow velocity increases, the pressure drop increases as well for all beta ratios. Finally, the discharge coefficient for each orifice plate was estimated and summarized in Table I.

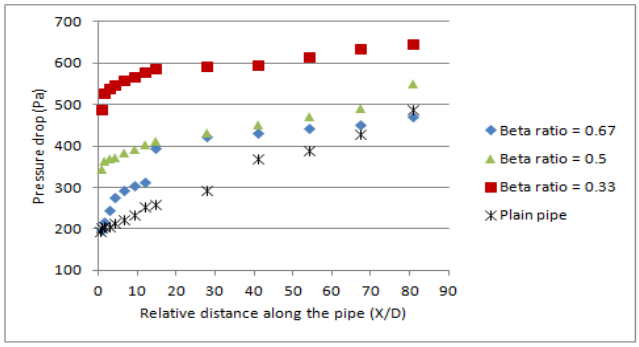

Fig. 6. Pressure drop along the pipe using circular orifices with different beta ratios at a motor speed of 1600 rpm.

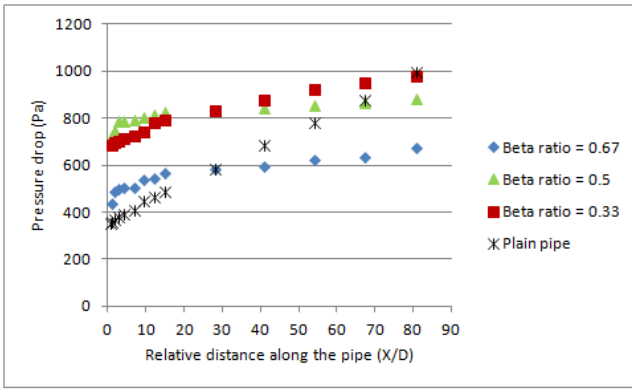

Fig. 7. Pressure drop along the pipe using circular orifices with different beta ratios at a motor speed of 2400 rpm.

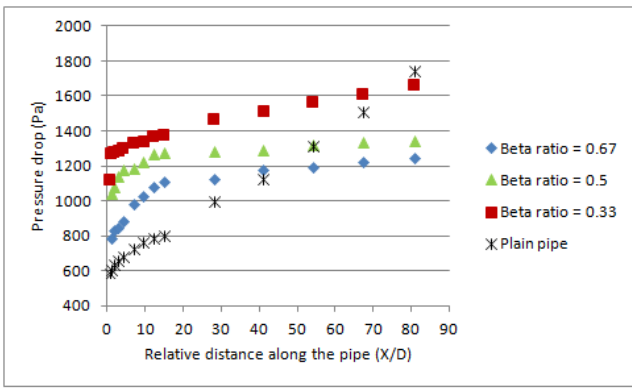

Fig. 8. Pressure drop along the pipe using circular orifices with different beta ratios at a motor speed of 3200 rpm.

TABLE I. DISCHARGE COEFFICIENTS FOR CIRCULAR ORIFICES

Orifice Diameter	*k*
50 mm orifice	0.608
38 mm orifice	0.604
25 mm orifice	0.599

The final group of experiments was performed using concentric triangular and square orifice plates that had the same flow area as the circular orifice plate of 25 mm in diameter. These experiments show the effect of the orifice shape on the pressure drop along the pipe. The results are illustrated in Figs. 9 to 11 for three different motor speeds. The figures show that the circular orifice gives less pressure drop than the other two orifices. At all considered motor speeds, the pressure drops caused by the triangular orifice and the square orifice were close to each other, with a slight increase in the pressure drop caused by the square orifice. It is clear that the pressure dropped sharply until approximately 20% of the pipe length, after which it became more flat in all cases.

International Journal of Engineering Research & Technology (IJERT)
ISSN: 2278-0181
Vol. 11 Issue 01, January-2022

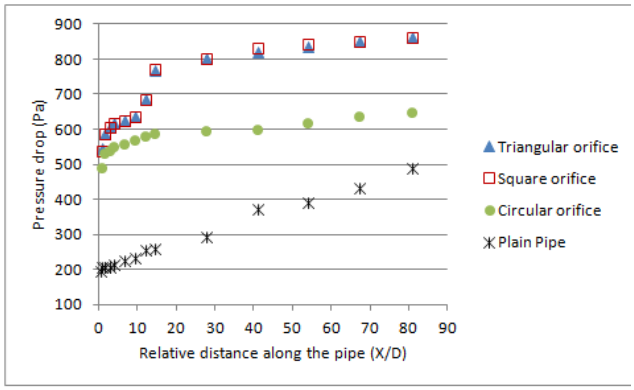

Fig. 9. Pressure drop along the pipe using different orifice shapes with the same flow area at a motor speed of 1600 rpm.

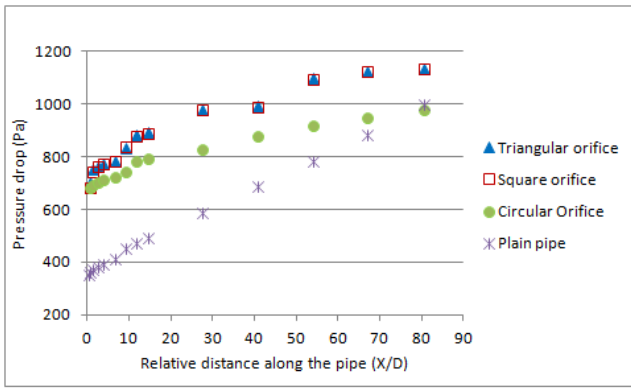

Fig. 10. Pressure drop along the pipe using different orifice shapes with the same flow area at a motor speed of 2400 rpm.

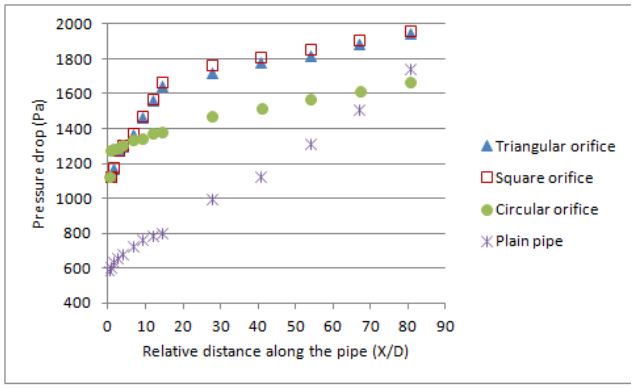

Fig. 11. Pressure drop along the pipe using different orifice shapes with the same flow area at a motor speed of 3200 rpm.

V. CONCLUSION

In this contribution, the turbulent airflow through a circular pipe has been investigated experimentally. In particular, the pressure drop along the pipe has been measured for various Reynolds numbers using a number of locally manufactured square-edged orifices of different sizes and shapes. The results confirmed that the pressure drop is directly proportional to the flow velocity. The results of the flow through circular orifices show that the pressure drop downstream of the orifices is inversely proportional to the beta ratio. The discharge coefficients for the different orifices have been estimated and found close to each other, with values ranging between 0.599 and 0.608. It is also found that the square orifice causes the highest pressure drop in comparison with triangular and circular orifices with the same flow area, with the triangular orifice coming second with pressure drop values close to those generated by the square orifice. The circular orifice produced the smallest pressure drop among the orifices.

REFERENCES

[1] D. S. Dhumal, Y. R. More, and U.S. Gawai, “Design, fabrication & CFD analysis of multi-hole orifice plate,” International Journal of Engineering Research & Technology (IJERT), vol. 6, issue 6, pp. 353-357, June 2017.

[2] H. Kim, T. Setoguchi, S. Matsuo,and S.R. Raghunathan, “Pressure drop control using multiple orifice system in compressible pipe flows,” Journal of Thermal Science ,vol. 10, issue 4, pp. 309-317, October 2001.

[3] A. Ahmadi, and S. B. M. Beck, “Development of the orifice plate with a swirler flow conditioner,” Sensor Review, vol. 25, issue 1, pp. 63-68, 2005.

[4] A. Abou El-Azm Aly, A. Chong, F. Nicolleau, and S. Beck, “Experimental study of the pressure drop after fractal-shaped orifices in a turbulent flow pipe,” International Journal of Mechanical and Mechatronics Engineering, vol. 2, issue 4, pp. 388-391, 2008.

[5] T. Zhao, J. Zhang, and L. Ma, “A general structural design methodology for multi-hole orifices and its experimental application,” Journal of Mechanical Science and Technology, vol. 25, issue 9, pp. 2237- 2246, 2011.

[6] E. Muñoz-Díaz, F. J. Solorio-Ordaz, and G. Ascanio, “A numerical study of an orifice flowmeter,” Flow Measurement and Instrumentation, vol. 26, pp. 85- 92, 2012.

[7] R. Kiš, M. Malcho, and M. Janovcova, “A CFD analysis of flow through a high-pressure natural gas pipeline with an undeformed and deformed orifice plate,” International Journal of Mechanical and Mechatronics Engineering, vol. 8, issue 3, pp. 606-609, 2014.

[8] B. Manshoor, M. F. Othman, I. Zaman, Z. Ngali, and A. Khalid, “Experimental study of various porosity of fractal flow conditioner for orifice plate flowmeters,” Applied Mechanics and Materials, vol. 699, pp. 915- 920, 2015.

[9] A. Dandwate, S. Mittal, O. Umale, P. Shelar, and R. Bajaj, “Effect of orifice plate shape on performance characteristics,” IOSR Journal of Mechanical and Civil Engineering, vol. 13, issue 4, pp. 50-55, July-August 2016.

[10] J. Likitha, T. M. Savitha, P. Kavya, G. Usha, and M. S. Karthik, “CFD analysis on different shapes of concentric orifice plate for turbulent flow,” International Journal of Engineering Research & Technology (IJERT), vol. 7, issue 6, pp. 421-426, June 2018.

[11] A. Bekraoui, A. Hadjadj, A. Benmounah, and M. Oulhadj, “Uncertainty study of fiscal orifice meter used in a gas Algerian field,” Flow Measurement and Instrumentation, vol. 66, pp. 200-208, 2019.

[12] British Standards 1042, Section 1.1.Measurement of Fluid Flow in Closed Conduits, 1992.